

## Article

# Belowground Structural Attributes and Morpho-Anatomical Response Strategies of *Bromus valdivianus* Phil. and *Lolium perenne* L. to Soil Water Restriction

Yongmei Zhang <sup>1</sup>, Javier García-Favre <sup>2</sup>, Haiying Hu <sup>3</sup>, Ignacio F. López <sup>4,\*</sup>, Iván P. Ordóñez <sup>5</sup>,  
Andrew D. Cartmill <sup>4</sup>, Vaughan Symonds <sup>4</sup> and Peter D. Kemp <sup>4</sup>

<sup>1</sup> State Key Lab of Aridland Crop Science, Gansu Agricultural University, Lanzhou 730070, China; zhangyongm@gsau.edu.cn

<sup>2</sup> Facultad de Agronomía, Universidad de la República, Montevideo 12900, Uruguay; jgfavre@fagro.edu.uy

<sup>3</sup> Science & Technology Department, Ningxia University, Yinchuan 750021, China; haiying@nxu.edu.cn

<sup>4</sup> School of Agriculture and Environment, Massey University, Palmerston North 4442, New Zealand; a.cartmill@massey.ac.nz (A.D.C.); v.v.symonds@massey.ac.nz (V.S.); p.kemp@massey.ac.nz (P.D.K.)

<sup>5</sup> Instituto de Investigaciones Agropecuarias, Kampenaike, Punta Arenas 6200000, Chile; ivan.ordonez@inia.cl

\* Correspondence: i.f.lopez@massey.ac.nz

**Abstract:** The effect of soil water restriction on the root structure and morpho-anatomical attributes of *Lolium perenne* L. (Lp) and *Bromus valdivianus* Phil. (Bv) was investigated. The anatomical structure of roots from plants grown under two water restriction conditions (20–25% and 80–85% field capacity (FC)) were assessed using paraffin embedding and thin sections. These sections were examined to assess anatomical traits, including root diameter (root D), stele diameter (stele D) and cortex thickness (cortex T), and xylem vessel of Lp and Bv roots. Tiller population, shoot herbage mass, and the shoot-to-root ratio were also determined. Under water restriction, biomass and tillers were significantly decreased ( $p < 0.001$ ), while the root-to-shoot ratio significantly increased, indicating a higher proportion of Bv roots than shoots when compared to Lp. The root D and stele D, and cortex T, were larger in Bv than in Lp ( $p < 0.001$ ), indicating a greater adaptation of Bv for water uptake and storage compared to Lp. Xylem vessels were wider in Lp when compared to Bv ( $p < 0.01$ ), indicating greater water flow within the plant. Water restriction generated a decrease in root D, stele D, and cortex T ( $p < 0.01$ ). Canonical variate analysis showed that the pith cell wall had a strong positive relationship with water restriction in both Bv and Lp; lignified xylem and the endodermis wall had a close relationship with Lp under water restriction. The findings demonstrate that Lp and Bv have individual structural and morpho-anatomical response strategies to increasing water restriction.

**Keywords:** drought; pasture brome; perennial ryegrass; root morphology



Academic Editor: Marzia Vergine

Received: 24 March 2025

Revised: 20 April 2025

Accepted: 23 April 2025

Published: 24 April 2025

**Citation:** Zhang, Y.; García-Favre, J.; Hu, H.; López, I.F.; Ordóñez, I.P.; Cartmill, A.D.; Symonds, V.; Kemp, P.D. Belowground Structural Attributes and Morpho-Anatomical Response Strategies of *Bromus valdivianus* Phil. and *Lolium perenne* L. to Soil Water Restriction. *Agronomy* **2025**, *15*, 1024. <https://doi.org/10.3390/agronomy15051024>

**Copyright:** © 2025 by the authors. Licensee MDPI, Basel, Switzerland. This article is an open access article distributed under the terms and conditions of the Creative Commons Attribution (CC BY) license (<https://creativecommons.org/licenses/by/4.0/>).

## 1. Introduction

Rising concentrations of greenhouse gases are projected to exacerbate climate change and increase the frequency, intensity, and severity of drought events [1–3], which represents a major challenge for agricultural production [4–6] as well as pasture growth, yield, and livestock performance [5,7,8]. Phenotypic plasticity of anatomical mechanisms may play a role in plant survival in response to water restrictions [9–11], in that plants show distinct responses to soil water restrictions through the expression of phenological and physiological plasticity and adjustment in their morpho-anatomical structures, with the effectiveness of soil water acquisition by fine roots representing a key mechanism for plant response

to periodic drought events [12–15]. Plant species differ in total and fine root biomass, root turnover, vertical root distribution, and maximum rooting depth [16,17], with deeper rooting depth associated with water-limited conditions [18,19].

Root structure and anatomy also vary among vascular plants [20,21], and are commonly investigated in soil water restriction studies due to their importance in drought survival [22–24]. Changes in root anatomy in response to soil water restriction include thickened root endodermis, pith, and sclerenchyma cells walls [25]. This reduction in thickness of the cortical parenchyma (through a reduction in cell size) reduces the diameter of primary xylem vessels, and generates an increase in the hydraulic resistance of roots, which lowers sap flow [26]. However, there is limited information on the relative effects of soil water restriction on the persistence, growth, and performance of grass species' root systems in temperate humid climates under these new climate conditions.

*Lolium perenne* L. (Lp) is a highly productive perennial grass of high quality and palatability [27,28], native to portions of Eurasia, North Africa and the Middle East, and is extensively cultivated in temperate humid climates for livestock production (e.g., Ireland, New Zealand, Chile, etc.). *Bromus valdivianus* Phil. (Bv), native to temperate humid regions of South America, is a deep-rooted, fast-growing, drought-tolerant perennial grass [9,29], with annual yield and herbage quality similar to Lp [28,30–32]. *Bromus valdivianus* has a greater tiller mass and leaf area, and a lower tiller number (per unit area) when compared to Lp [9,22,33]. In the south of Chile, highly productive pastures of these species form and persist as naturalised swards [33]. Under water restriction, Lp and Bv have exhibited different growth strategies, based on physiological regulation of the tiller population, lamina growth, and root mass [22,34]. However, there is limited information on the adaptive morphological and anatomical traits of Bv and Lp in response to drought. *Lolium perenne* and Bv, through different morphological traits, have been reported to adjust their individual tissues and cells in aboveground parts to reduce water loss [35]. In general, below-ground plant response to water restriction, the physiological and cellular properties and their relationships to morpho-anatomical characteristics, which regulate water uptake and movement, are not well understood [10,11,36]. Thus, understanding Lp and Bv's response to water restriction is an important aspect of adapting livestock production to climate variability, thereby maintaining long-term profitability from resilient agroecosystems [37].

The hypothesis of this study was that Lp and Bv roots have distinct structural attributes and anatomical adjustments that promote survival under soil water restriction. Therefore, the objectives were to: (i) Examine and analyse the morpho-anatomical traits of the Bv and Lp roots when grown under soil water-limiting conditions; and (ii) Investigate the role of these structural root adjustments for the maintenance of plant water flow and reduction of plant water loss.

## 2. Materials and Methods

### 2.1. Experimental Design and Treatments

The experiment was performed under glasshouse conditions, at Massey University's Plant Growth Unit (40.37° latitude south and 175.61° longitude west), Palmerston North, New Zealand, between September 2018 and March 2019. The average daily temperature, relative humidity, and PAR were ~22.2 °C, 60.2%, and 84.1  $\mu\text{mol m}^{-2} \text{s}^{-1}$ , respectively.

Containers (400 cm<sup>3</sup>; 20 × 20 cm) were filled with 3.8 kg of dry substrate (30% Manawatu silt loam soil and 70% fine sand by volume). The nutrient concentration and chemical status of the substrate were: pH 6.3 (soil: water = 1:2), 35 Olsen-P mg L<sup>-1</sup>, 0.34 exchangeable K mEq 100 g<sup>-1</sup>, 2.4 exchangeable Ca me 100 g<sup>-1</sup>, 0.60 exchangeable Mg mEq 100 g<sup>-1</sup>, <0.05 exchangeable Na mEq 100 g<sup>-1</sup>, 3.0 CEC me 100 g<sup>-1</sup>, and 83 SO<sub>4</sub><sup>2-</sup> mg kg<sup>-1</sup>. Based on the nutrient concentration, every 30 kg of the substrate were applied 60 g of slow-release

fertiliser (14% nitrogen (N), 5% phosphorus, 10% soluble potash, 0.5% magnesium, 3.2% sulphur, 1.6% iron and 0.3% manganese), 30 g of short-term fertiliser (14% total N, 6% phosphorus, 11.6% potassium, 1% magnesium, 4% sulphur, 1% iron and 0.5% manganese) and 45 g of dolomite.

Two seeds of *Bromus valdivianus* Phil. cv. Bareno were sown in the centre of half of the pots, and two seeds of *Lolium perenne* L. cv. Trojan (Barenbrug, Christchurch, New Zealand) were sown in the centre of the remaining pots on 23 September 2018. Between sowing and the establishment of the water supply treatments (12 weeks) the soil was maintained at 80–85% of the FC (volumetric soil water content (VWC)). After seedling emergence, seedlings were thinned to one seedling per pot (3 October 2018).

To determine the field capacity (verified at 16% of VWC at 33 kPa of matric potential) and permanent wilting point (PWP; verified at 2% VWC at 1543 kPa of matric potential) for the substrate utilised, the water retention curve was calculated. Therefore, three undisturbed soil samples were collected using a 100 cm<sup>3</sup> metallic cylinder. Based on VWC the water supply treatments were established between 80–85% of the total FC [FC–80–85% (FC–PWP)] for the control treatment; 20–25% of the total FC [FC–20–25% (FC–PWP)] for the water restriction treatment. Thereafter, the water column was calculated (see Equation (1)) to maintain the pots at their respective VWC. The substrate water restriction levels resulted in 13.2–14% VWC for the control treatment, and 4.8–5.5% VWC for the water restriction treatment.

The experimental design was a randomised complete block design (five blocks), with factorial distribution of the treatments [38], two species (Lp and Bv), and two levels of soil water supply (control and water restriction) (two species x two levels of water supply x five blocks). The water restriction period ran between 23 December 2018 and 17 January 2019. Five additional blocks were grown and treated in the same manner as the study pots, to utilise them for daily soil substrate TDR measurements (Mini Trace with soil-moisture TDR Technology, Soil Moisture Equipment Corp., Goleta, CA, USA), so that the soil of the study plots was not disturbed by the TDR rods, and the daily water loss and water volume required to replace the water lost per pot could be determined, such that each pot was maintained within the range of its water restriction treatment, as described by [9,35,39]. The volume of water added daily was calculated using the following formula:

$$I = \frac{IC - WC}{100} \times SW \quad (1)$$

where I is irrigation (kg); IC is the irrigation criteria (% in volume); WC is the substrate soil water content (% in volume); and SW is the substrate soil's dry weight (kg).

## 2.2. Shoot and Root Sample Collection

The evaluation of the effect of the soil water restriction on the plants' roots and shoots was performed 25 days after the start of the water treatment application. The evaluation of shoots focused on tiller number (block,  $n = 5$ ) and herbage mass per plant, which were recorded. The root mass was carefully collected, washed, and handled to avoid any loss of root material. Herbage and root mass were then oven-dried at 70 °C for at least 72 h. Shoot biomass, root dry mass (DM), and the root-to-shoot ratio (block,  $n = 5$ ) were then determined.

At harvest, root samples from each plant were divided into two portions taken from the root collar down. Root segments measured from the root collar down were separated into segments between 4–5 cm [lower roots (LR)] and segments between 2–3 cm [upper roots (UR)]. All samples were fixed in F.A.A. solution (70% ethanol: glacial acetic acid: formaldehyde in a 90:5:5 ratio by volume) immediately after collection [40]. Root diameter

(or root D), stele diameter (or stele D), xylem diameter (or xylem D), and the width of the epidermis, cortex thickness (or cortex T), tracheary element, pericycle, endodermis, endodermis wall, pith, pith wall, aerenchyma, epidermis, pericycle, periderm, and root hair number were measured ( $\mu\text{m}$ ) and evaluated.

### 2.3. Paraffin Sections

The samples were fixed in F.A.A solution for 24 h, then removed and rinsed twice with 50% isopropanol for 45 min. The method described by [41] was used to process the samples as they were dehydrated in 70%, 85%, and 95% isopropanol (including 1% eosin) at room temperature for 45 min. The absolute dehydration of the samples was obtained when the samples were dipped three times for 30 min in 100% isopropanol. The transparency of the samples was reached by a diminishing gradient of isopropanol and increasing levels of mineral oil for 30 min at 60 °C or until 100% of the mineral oil had completely entered the sample. Then, the mineral oil that was inside the samples was replaced with paraplast X-tra. Paraplast X-tra replacement was repeated five times every 2.5–3 h at 60 °C, after which the samples were stored in paraplast X-tra before embedding.

Root samples of the same treatment were embedded (Leica HistoCore Arcadia with Arcadia H and Arcadia C, Leica biosystems, Mt Waverly, VIC, Australia) in long, thin boats filled with 62 °C paraffin. Solidified paraffin blocks were then clipped and pasted into microtome cartridges using hot paraffin. The rotary microtome (Leica RM2265, Leica Biosystems, Mt. Waverly, VIC, Australia) cut down sections at 8  $\mu\text{m}$ , 10  $\mu\text{m}$ , or 15  $\mu\text{m}$  thickness. Sections were collected on microscope slides, dried at 40 °C for ~72 h, stained in safranin for 9 h, and re-dyed in fast green for 20 s. An Olympus BX51 microscope (Mt. Waverley, VIC, Australia) was used to examine the sections. The images were captured via CCD (Olympus SC30, Mt. Waverley, VIC, Australia), and the structures in them were measured (cellSens 2.1 Software, Olympus, Mt. Waverley, VIC, Australia).

### 2.4. Statistical Analysis

The normal distribution and homogeneity of variance of the data were analysed using Kolmogorov–Smirnov and Bartlett’s tests before ANOVA with the GLM procedures applied. Fisher’s Least Significant Difference (LSD) was used to explore differences among treatment means. To perform canonical variate analysis (CVA) [42], variables were standardised using the following equation:

$$Z = (y_i - \bar{y}) / \text{St.Dev.} \quad (2)$$

where Z is the standardised variable; y is the original variable;  $\bar{y}$  is the mean; and St. Dev. is the standard deviation [9]. All statistical analyses were performed using SAS (Statistical Analysis System) software version 9.2 (SAS Institute, Inc., Cary, NC, USA).

## 3. Results

### 3.1. Root and Shoot Biomass

The tiller number ( $\times 2.5$ ) per plant was significantly higher ( $p < 0.001$ ) in Lp compared to Bv. For both species the water restriction decreased the tiller number significantly ( $p < 0.001$ ) from 48 to 23.8 in Bv and from 122.8 to 60.4 in Lp. The shoot and root mass decreased for both species, leading to a significantly higher root-to-shoot ratio for Bv, from 0.29 to 0.47 ( $p < 0.05$ ), while Lp’s root-to-shoot ratio remained statistically similar for both soil water restriction levels. For more detailed information on the effect of the soil water restriction on shoot attributes of Bv and Lp, please refer to [35].

### 3.2. Traits and Adjustments of *Bromus valdivianus* and *Lolium perenne*

All of the anatomical root traits of Bv were significantly ( $p < 0.05$ ) different from those of Lp (Tables 1 and 2). *Bromus valdivianus* root D and stele D were significantly larger ( $p < 0.001$ ) than those in Lp. The *Bromus valdivianus* cortex, tracheary element, pericycle, and endodermis were significantly thicker ( $p < 0.001$ ) when compared to Lp. *Lolium perenne*'s xylem D was significantly wider ( $p < 0.01$ ) (7.96 and 7.55  $\mu\text{m}$  in UR and LR, respectively) when compared to that of Bv (6.82 and 5.49  $\mu\text{m}$  in UR and LR, respectively) (Tables 1 and 2). Xylem D significantly increased from 5.79  $\mu\text{m}$  to 7.86  $\mu\text{m}$  in Bv UR (Table 1) and decreased from 5.91  $\mu\text{m}$  to 5.07  $\mu\text{m}$  in Bv LR (Table 2). Between the species, xylem D showed greater size in Lp roots when compared to Bv, in both UR and LR (Tables 1 and 2).

Water restriction treatments affected the anatomical structures of LR when compared to UR (Table 1 vs. Table 2). Root D, stele D, cortex T, the tracheary element, the endodermis ( $p < 0.001$ ), the pericycle ( $p < 0.01$ ), and the pith cell wall ( $p < 0.05$ ) significantly decreased in UR under water restriction when compared with the control treatment (Table 2). There were no significant differences in the same tissues and cells in the LR (Table 1).

Under soil water restriction, root D and stele D decreased in size in LR (Table 2). The thickness of the endodermis decreased, while the cortex and endodermis cell wall were not affected in UR ( $p > 0.05$ ). The pith cell wall became thicker ( $p < 0.05$ ) (Tables 1 and 2), which was especially so in UR for Bv but not for Lp (Table 2).

Individual roots anatomical traits for Bv and Lp were observed. In Lp UR, the periderm had 3–4 layers and an aerenchymatous cortex (Figure 1E–G). Aerenchyma structures were found in Lp UR, and when compared to Bv roots, the tracheary, in the stele, were bigger and more abundant when compared to Lp (Figure 1A,B vs. Figure 1E,F; Figure 2A,B vs. Figure 2C,D). Xylem vessels in Lp were wider than in Bv (Figure 1F vs. Figure 1B; Figure 2D vs. Figure 2B). Cortex cell layer numbers in both UR and LR were greater in Bv when compared to Lp (Figure 1A vs. Figure 1E; Figure 2A,B vs. Figure 2C,D).

Soil water restriction resulted in changes in the anatomical root structures of Bv and Lp, in that both Bv's and Lp's root cross-section shapes became more irregular due to cortex cell deformation (Figure 1C vs. Figure 1A,G vs. Figure 1E; Figure 2E vs. Figure 2A). This was especially obvious in UR (Figure 1C,G). In Lp roots, the wall of pith cells was strengthened with lignification, cutinisation, and/or suberification (xylem was dyed red by safranin) (Figure 1H vs. Figure 1F). In Bv roots, the cortex layer was reduced from 7–9 in the well-watered control treatment to 4–5 layers in the water-restricted treatment (Figure 1C,D vs. Figure 1A,B; Figure 2E,F vs. Figure 2A,B).

### 3.3. Canonical Variate Analysis of Anatomical Root Structures

The soil water restriction–species interaction effects expressed on the species anatomical root traits were analysed via canonical variate analysis (CVA) (Figure 3), which explained 92% of the variation of the analysed variables, such that CAN 1 explained 73.4% and CAN 2 18.6% with a significant Wilks' Lambda ( $p < 0.0001$ ; Figure 3). CAN 1 indicated differences between species in terms of anatomical traits in UR (Figure 3A,B), in that Bv had a positive relationship with increasing root D, stele D, cortex T, tracheary element, endodermis, and pericycle, constituting a contrast with increasing pith size that was closely related to Lp. CAN 2 showed differences between the species due to water treatments, especially between the 80% FC and 20% FC in UR anatomical variables. Increasing root D, stele D, and the width of the epidermis, pericycle, and endodermis were associated with a water condition of 80% FC, in contrast with increasing the width of the pith cell wall and tracheary element, which had a strongly positive relationship with soil water restriction (20% FC) in Bv and to a lesser extent in Lp UR (Figure 3C).

**Table 1.** Root and stele diameter, thickness of endodermis, cortex, pith, endodermis cell wall and pith cell wall, the width of the tracheary element, xylem, endodermis, pericycle in upper root (UR; between 2–3 cm from the root collar) in *Bromus valdivianus* (Bv) and *Lolium perenne* grown (Lp) at 80~85% field capacity (FC) and 20~25% FC. The data are expressed as mean ± sem at 5 blocks. (Unit: µm).

	Root Diameter	Stele Diameter	Epidermis Thickness	Cortex Thickness	Tracheary Element	Xylem Diameter	Pericycle Thickness	Endodermis Thickness	Endodermis Wall	Pith Thickness	Pith Wall
	Species										
Bv	441.25 ± 10.13	199.01 ± 2.56	15.48 ± 0.96	105.45 ± 3.73	20.45 ± 0.39	6.82 ± 0.19	11.99 ± 0.57	10.22 ± 0.35	2.55 ± 0.14	32.03 ± 1.50	4.24 ± 0.15
Lp	325.55 ± 13.01	146.54 ± 4.83	8.07 ± 0.62	69.86 ± 4.05	14.76 ± 0.84	7.96 ± 0.19	7.89 ± 0.46	5.56 ± 0.40	2.05 ± 0.08	53.36 ± 2.89	3.72 ± 0.14
Significance	***	***	***	***	***	**	***	***	*	***	***
	Soil water content										
80–85% FC	392.03 ± 16.69	176.60 ± 7.32	12.23 ± 0.71	88.25 ± 5.44	16.88 ± 0.99	6.88 ± 0.22	10.63 ± 0.72	8.12 ± 0.69	2.34 ± 0.11	44.96 ± 3.11	3.73 ± 0.12
20–25% FC	374.76 ± 14.61	168.95 ± 4.29	11.33 ± 1.42	87.06 ± 4.98	18.33 ± 0.66	7.89 ± 0.18	9.26 ± 0.48	7.66 ± 0.41	2.25 ± 0.13	40.43 ± 3.66	4.23 ± 0.14
Significance	ns	ns	ns	ns	ns	**	*	**	ns	ns	*
	Species × Soil water content										
Bv × 80–85% FC	455.50 ± 13.70	209.79 ± 2.34 a	14.93 ± 0.98	108.06 ± 4.69	20.83 ± 0.59 a	5.79 ± 0.16 b	13.63 ± 0.68 a	11.30 ± 0.37 a	2.64 ± 0.16	30.36 ± 1.62 c	3.73 ± 0.17
Bv × 20–25% FC	427.00 ± 14.39	188.23 ± 2.11 b	16.04 ± 1.55	102.84 ± 5.68	20.07 ± 0.50 a	7.86 ± 0.23 a	10.36 ± 0.66 b	9.14 ± 0.36 b	2.46 ± 0.24	33.69 ± 2.48 c	4.75 ± 0.16
Lp × 80–85% FC	328.57 ± 20.64	143.41 ± 8.50 c	9.52 ± 0.75	68.43 ± 6.12	12.94 ± 1.20 c	7.98 ± 0.32 a	9.63 ± 0.75 c	4.94 ± 0.61 d	2.05 ± 0.09	59.56 ± 3.71 a	3.74 ± 0.14
Lp × 20–25% FC	322.53 ± 15.98	149.66 ± 4.91 c	6.62 ± 0.29	71.28 ± 5.50	16.58 ± 1.09 b	7.93 ± 0.24 a	8.16 ± 0.55 c	6.19 ± 0.52 c	2.04 ± 0.12	47.16 ± 4.69 b	3.71 ± 0.19
Significance	ns	**	ns	ns	*	**	**	***	ns	*	ns

Letters that differ within the same column indicate statistically significant values at \*  $p \leq 0.05$ ; \*\*  $p \leq 0.01$ ; \*\*\*  $p \leq 0.001$ ; ns  $p > 0.05$ . FC, field capacity; Bv, *Bromus valdivianus*; Lp, *Lolium perenne*.

**Table 2.** The root and stele diameter, thickness of peridermis, cortex, pith, pericycle cell wall and pith cell wall, the width of tracheary element, xylem, endodermis, pericycle in lower roots (LR; 4–5 cm from the root collar) in *Bromus valdivianus* and (Bv) *Lolium perenne* (Lp) grown at 80~85% field capacity (FC) and 20~25% FC. The data are expressed as mean ± sem at 5 replications. (Unit: µm).

	Root Diameter	Stele Diameter	Epidermis Thickness	Cortex Thickness	Tracheary Element	Xylem Diameter	Pericycle Thickness	Endodermis Thickness	Endodermis Wall	Pith Thickness	Pith Wall
	Species										
Bv	403.90 ± 12.88	158.86 ± 2.72	13.13 ± 0.44	108.66 ± 4.14	18.23 ± 0.27	5.49 ± 0.13	12.07 ± 0.46	9.62 ± 0.37	0.89 ± 0.09	45.16 ± 2.17	5.14 ± 0.10
Lp	293.86 ± 9.32	125.26 ± 6.83	11.73 ± 0.52	73.48 ± 2.95	10.52 ± 1.00	7.55 ± 0.28	8.59 ± 0.38	6.50 ± 0.41	1.36 ± 0.13	44.65 ± 2.62	4.83 ± 0.12
Significance	***	***	ns	***	***	***	***	***	*	ns	ns
	Soil water content										
80–85% FC	398.59 ± 14.17	159.33 ± 4.54	14.13 ± 0.48	106.34 ± 4.50	15.98 ± 0.75	6.60 ± 0.27	11.31 ± 0.56	9.35 ± 0.45	1.21 ± 0.12	46.97 ± 2.27	4.77 ± 0.10
20–25% FC	299.18 ± 8.48	124.79 ± 5.13	10.73 ± 0.65	75.80 ± 3.02	12.77 ± 1.02	6.44 ± 0.25	9.36 ± 0.38	6.77 ± 0.38	1.04 ± 0.12	42.84 ± 2.49	5.21 ± 0.11
Significance	***	***	ns	***	***	ns	**	***	ns	ns	*
	Species × Soil water content										
Bv × 80–85% FC	473.7 ± 9.4 a	168.2 ± 2.41 a	12.02 ± 0.64	130.2 ± 3.62 a	18.45 ± 0.30 a	5.91 ± 0.19 b	13.30 ± 0.63	10.87 ± 0.42	1.11 ± 0.11	51.52 ± 2.91	4.64 ± 0.11 b
Bv × 20–25% FC	334.1 ± 7.2 b	149.5 ± 4.49 b	14.25 ± 0.45	87.1 ± 2.45 b	18.01 ± 0.54 a	5.07 ± 0.17 c	10.85 ± 0.32	8.37 ± 0.30	0.68 ± 0.15	38.79 ± 2.85	5.65 ± 0.13 a
Lp × 80–85% FC	323.5 ± 14.8 b	150.4 ± 11.34 b	16.25 ± 0.43	82.5 ± 3.89 b	13.51 ± 1.78 b	7.29 ± 0.51 a	9.32 ± 0.71	7.84 ± 0.66	1.30 ± 0.33	42.43 ± 3.05	4.89 ± 0.17 b
Lp × 20–25% FC	264.28 ± 7.6 c	100.1 ± 4.02 c	7.21 ± 0.77	64.5 ± 2.86 c	7.53 ± 0.22 c	7.81 ± 0.22 a	7.87 ± 0.37	5.16 ± 0.45	1.41 ± 0.13	46.88 ± 3.71	4.77 ± 0.16 b
Significance	**	**	ns	**	**	*	ns	ns	ns	ns	**

Letters that differ within the same column indicate statistically significant values at \*  $p < 0.05$ ; \*\*  $p < 0.01$ ; \*\*\*  $p < 0.001$ ; ns  $p > 0.05$ . FC, field capacity; Bv, *Bromus valdivianus*; Lp, *Lolium perenne*.

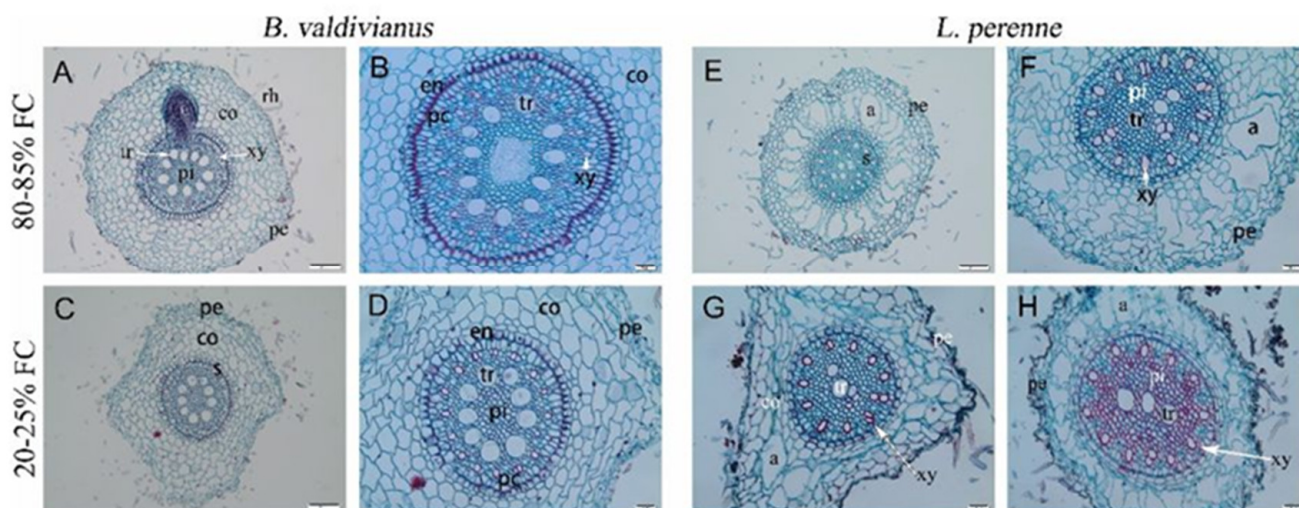


**Figure 1.** Anatomical structure of the upper root (UR) in *Bromus valdivianus* (Bv) and *Lolium perenne* (Lp) exposed to different water restrictions with (A–D), Bv; (E–H), Lp. Row 1 represents under 80–85% field capacity (FC), row 2 under 20–25% FC. Bars: 10  $\mu\text{m}$  in (A,C,E,G); 20  $\mu\text{m}$  in (B,D,F,H). The letters within the images are: a, aerenchyma; co, cortex; en, endodermis; pc, pericycle; pe, periderm; pi, pith; rh, root hair; s, stele; tr, tracheary element; xy, xylem.

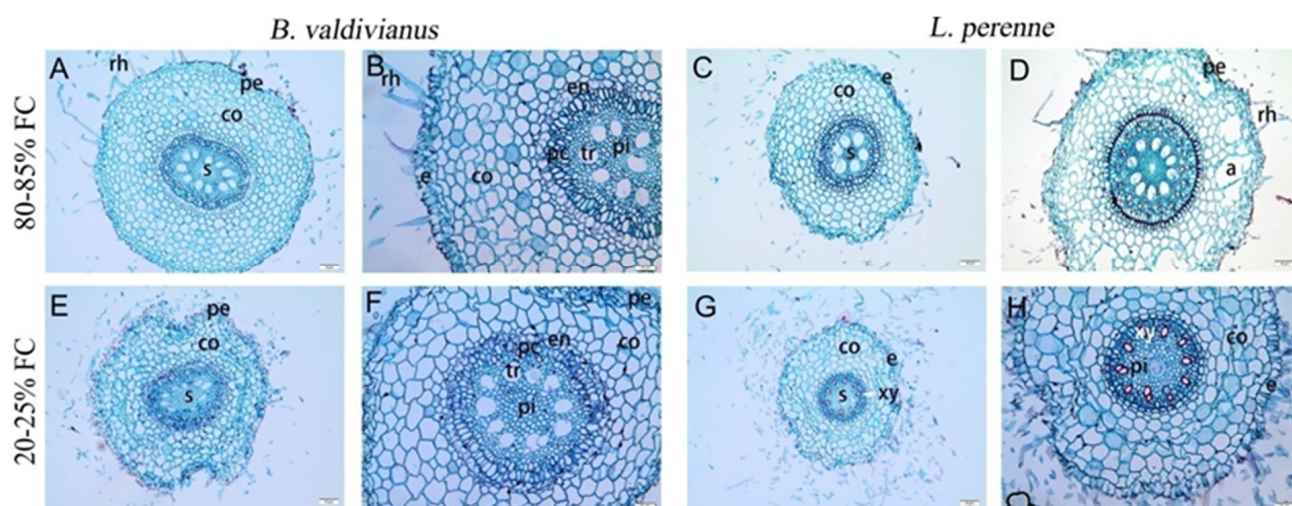


**Figure 2.** Anatomical structure of the lower root (LR) in *Bromus valdivianus* (Bv) and *Lolium perenne* (Lp) exposed to different water restrictions. Left four images are Bv; Right four images Lp. Row 1 represents under 80–85% field capacity (FC), Row 2 under 20–25% FC. Bars: 10  $\mu\text{m}$  in (A,C,E,G); 20  $\mu\text{m}$  in (B,D,F,H). The letters within the images are: a, aerenchyma; co, cortex; e, epidermis; en, endodermis; pc, pericycle; pe, periderm; pi, pith; rh, root hair; s, stele; tr, tracheary element; xy, xylem.

In LR, the canonical variate analysis explained 97.6% of the variation between the variables, in which CAN 1 explained 78.7% ( $p < 0.001$ ) and CAN 2 18.9% ( $p < 0.05$ ) with a highly significant Wilks' Lambda ( $p < 0.0001$ ; Figure 4). CAN 1 indicated mainly interspecies differences between Bv and Lp in terms of anatomical traits in the LR (Figure 4A,B). Greater root D, stele D, periderm, cortex T, tracheary element, endodermis and pericycle variables were related with Bv species, especially when Bv was at 80% FC, due to their small dimensions when Bv was at 20% FC. CAN 1 indicated a contrast between Bv and Lp, such that root D, stele D, the periderm, cortex T, tracheary element, endodermis and pericycle were larger in Bv and decreased in size for Lp. However, the contrary was found for Lp with the endodermis wall, pith wall, and red xylem (lignified xylem) width in relation to Bv (Figure 4B) at any of the soil water restriction levels.

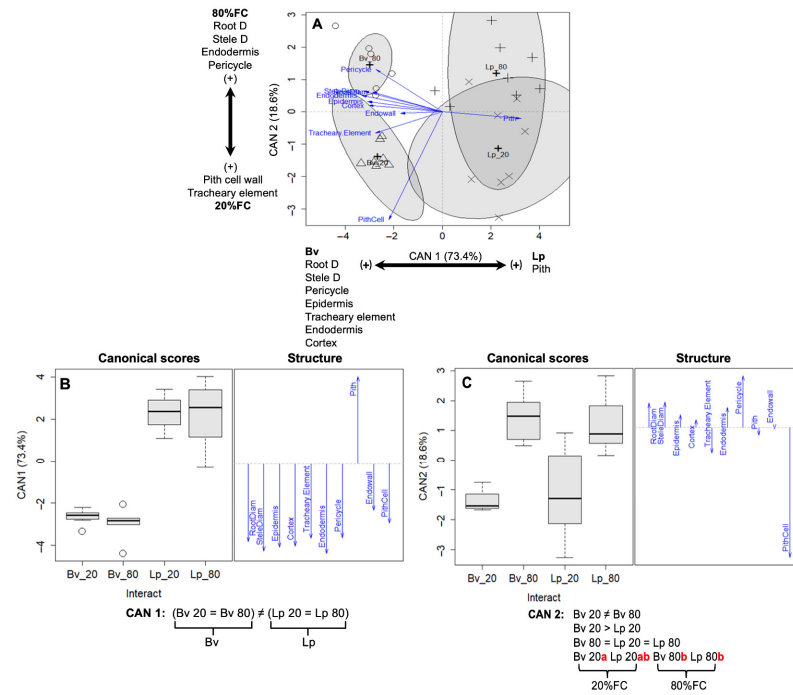


**Figure 3.** Canonical variate analysis for upper root (UR) anatomical structure in *Bromus valdivianus* (Bv) and *Lolium perenne* (Lp) grown at 80–85% field capacity (FC) and 20–25% FC. (A): CAN 1 and CAN 2 explained 92% of the variation among the variables and interaction of species and water restriction; (B): CAN 1 explained 73.4%; (C): CAN 2 explained 18.6%. Vectors indicated variables of anatomical structure. Oval highlighted the 95% confidence interval around the means for the interaction of species and water restriction.

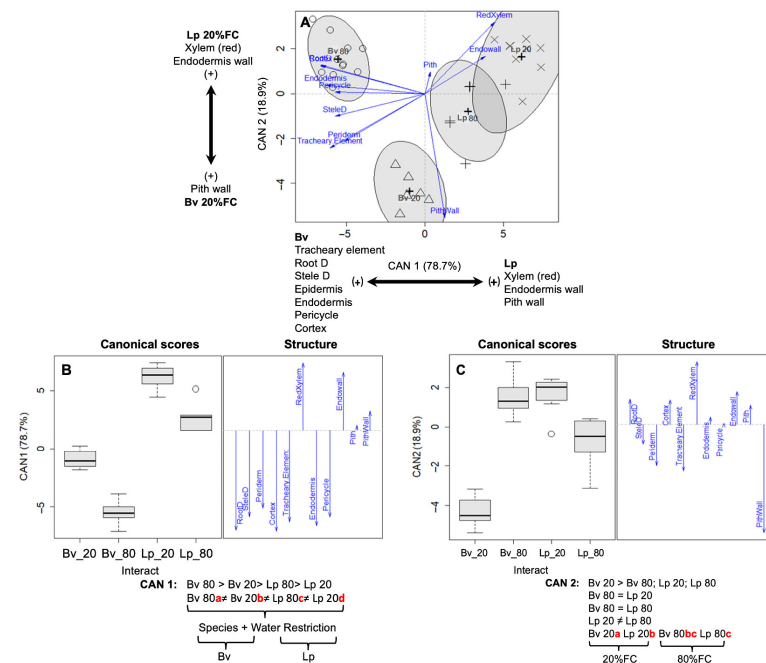


**Figure 4.** Canonical variate analysis for lower root (LR) anatomical structure in *Bromus valdivianus* (Bv) and *Lolium perenne* (Lp) grown at 80–85% field capacity (FC) and 20–25% FC. (A): CAN 1 and CAN 2 accounted for 97.6% of the variation among the variables and interaction of species and water restriction; (B): CAN 1 explained 78.7%; (C): CAN 2 explained 18.9%. Vectors indicated variables of anatomical structure. Oval highlighted the 95% confidence interval around the means for interaction of species and water restriction.

The effects of soil water restriction on the LR anatomical variables of Bv and Lp were accounted for by CAN 2. *Bromus valdivianus* adjustments in the LR anatomy were expressed through a greater pith wall width (21.8%), and the diminishment of the red xylem (−14.2%) and endodermis wall (−38.7%) with increased soil water restriction. Soil water restriction resulted in few changes in Lp's LR anatomical variables, especially CAN 2, illustrating the contrast between Bv's and Lp's response to water restriction (Figure 4A,C). At 20% FC, Bv had a strong positive relationship between LR increased pith cell wall width, while for Lp, the red xylem and the endodermis wall width increased (Figure 4C).

#### 4. Discussion

The anatomical responses of plant roots to short- or long-term water restriction are diverse and depend on adaptive characteristics expressed through an array of resistance mechanisms [43,44], including adaptations related to plant physiology [45], morphology [22], metabolism [46], and anatomic modifications [14]. Plants' anatomical adaptations are highly relevant for water movement and retention within plant tissue. Plants' responses include absorption of water from the soil, maintaining plant/organ water status, turgor, and water flow continuity through the organs (lateral short-distance or longitudinal long-distance water movement), while minimising leaf and shoot water loss. Soil water restriction results in root tissue dehydration, which drives a plant's resistance/avoidance response to soil water deficit, e.g., a prolific root system, and root-to-shoot ratio increase to facilitate water absorption [21,22]. Plants' root response to drought varies and includes anatomical adjustments and modifications of root anatomy, which facilitates water absorption and increases the survival probabilities of individual plants [47].

##### 4.1. Morpho-Anatomical Root Traits and Adjustments to Water

*Bromus valdivianus* had a larger root D, indicating a stronger water absorption power [48,49] and showed a thicker root cortex, which may contribute to stronger water retention capacity in comparison to Lp. This suggests that the cortex parenchyma cells may serve as a tissue "collecting" ion [50–52], and drive/modulate apoplastic and symplastic water transport and/or storage [53], which are important for long-distance solute transport and maintenance of plant water status [50].

The root's epidermis width diminished in Lp (UR −30%; LR −55.6%) and increased in Bv (UR +7.4%; LR +18.6%), suggesting a more difficult water flow within the root via the epidermis in Lp under high soil water potential (i.e., soil water restriction). The outermost layer of the root (epidermis or periderm) is the area of water and non-selective mineral intake (apoplastic) [54]. This would support the greater photosynthetic activity and lower osmotic and water potential of Bv when compared to Lp during water restriction periods [32].

The periderm serves as a protective layer in plant roots, and is formed from secondary vascular tissue [40]. The periderm had 3–4 layers in Lp UR and an aerenchymatous cortex, similar to roots found in species that colonise wetlands ecosystems [55]. Aerenchyma was observed in Lp UR and LW in the control treatment and contained enlarged air spaces produced by tearing or dissolution of the cortex cell walls [56]. The Oxygen (O<sub>2</sub>) from above-ground tissues, which is not consumed in respiration, is transported to the aerenchyma in the roots, facilitating O<sub>2</sub> release to the root tips and other plant organs under waterlogged conditions [55,57,58], thereby enabling plants to tolerate and survive in flooded environmental conditions. The aerenchyma observed in Lp roots in the study may play a significant role in agronomic parameters, such as net primary production, as Lp showed greater pasture growth and better physiological responses under waterlogged conditions (during winter) than Bv [34].

#### 4.2. Modification of Morpho-Anatomical Traits of the Root Relevant to Water Movement

Water restriction affected the anatomical structure of the root in both Bv and Lp, in that root D, cortex thickness (in LR) and stele D decreased under water restriction when compared with the control water treatment, which may have weakened water uptake and flow. Thinner roots have a smaller root surface area, which means less opportunity to capture water in the soil, resulting in reduced water uptake, especially when the diminishment of root D is associated with a diminishment of stele D (i.e., diminishment of the water movement capacity) [59]. In absorptive roots, a reduced cortex-to-stele ratio is advantageous under dry conditions for water and nutrient movement, due to a greater proportion of stele diameter (which enhances water transport capacity) relative to cortex thickness (which reduces resistance to water flow into the root) [59]. Hence, based on the data from Tables 1 and 2, the cortex thickness-to-stele diameter ratio indicates that the upper root (UR) sections have a thicker cortex relative to each micron of stele diameter (Bv = 1.89; Lp = 2.10) compared to the lower root (LR) sections (Bv = 0.68; Lp = 0.60). This suggests that the LR sections have a greater capacity for water uptake and transport than the UR sections. However, a decrease in root diameter would increase the matric potential within the root, which may increase the water uptake at high soil matric potential. Therefore, Lp should show a greater capacity of water uptake under water restriction due to its thinner roots. In this context, differences in soil matric potential between Lp pastures and diverse pastures at the soil surface were observed, suggesting that Lp has a greater capacity to uptake water under higher soil matric potential periods (i.e., water restriction) [29,37].

We suggest, based on current understanding of root stele anatomy and physiology, that apoplast canal theory [60] explains solute and water transport. In that, stele D was reduced under water stress in Bv and Lp, which probably restrained water flow in stele long-distance transportation to leaf and leaf-sheath. Decreasing water supply to leaves may decrease shoot biomass under water restriction, resulting in stomata closure, reduced transpiration and water loss [15,61], and a reduction in the root-to-shoot ratio. Total biomass reduction and increased root-to-shoot ratio, reduced water loss (shoot reduction), and enhance water uptake potential (root growth/maintenance), suggesting that plants allocate resources to roots and/or maintain root mass during periods of water restriction [22]. The water restriction tolerance of Bv compared to that of Lp was demonstrated through the greater increase ( $p < 0.05$ ) of Bv root-to-shoot ratio (62% increased) when compared to Lp (21.4% increased), which was accompanied by a thicker cortex (higher number of cortex cell layers) ( $p < 0.01$ ) in Bv LR. Other studies have reported a greater increase of Bv roots when compared to Lp with increasing soil water restriction [9,31,34].

Increasing root-to-shoot ratio in arid environments has been observed and reported in a variety of plant species, for example soybean (*Glycine max* L.) [10], rice [62], cotton (*Gossypium hirsutum* L.) [63], and tall fescue (*Lolium arundinaceum* (Schreb.) Darbysh. subsp. *arundinaceum*; sin. *Festuca arundinacea* Schreb.) [64]. Tall fescue drought tolerant germplasm was reported to have a high root-to-shoot ratio, which is an important parameter for ecotypes selection for improving drought tolerance in arid environments [65]. In the present study, the observed diminishment of Bv root cortex and Bv shoot vascular bundle [35] in response to water restriction suggests that this species increases root-to-shoot ratio to enhance its tolerance to water-stress conditions [66] and from an anatomical perspective, reduces transpiration through reduction of leaf area [22,66].

From the result of UR and LR CVA of anatomical structure, it was found that the increase of the pith cell wall thickness was related to drought tolerance in Bv, while the endodermal cell wall, xylem vessel, pith cell wall, and lignification of the pith cell wall were related to drought tolerance in Lp. Thickening of the pith cell wall played an important role in the drought resistance in Bv and Lp grasses species. In that, pith tissue, composed of

tightly packed parenchyma cells in the centre of the stele, were simple metabolically active cells, capable of dividing, and bounded by a primary cell wall, which may be involved in root respiration, storage, and secretion [53]. Under the dry condition of 20–25% FC, pith tissue in Bv and Lp was lignified (Figure 1H) or thickened into sclerenchyma, due to the plasticity of parenchyma cells, which allows for a change in physiological function related to water status, from water storage to long-distance water transport [53].

In Lp the xylem vessel and endodermal cell wall were positively linked to dry conditions (Figure 4). The xylem consisting of water-conducting sclerenchyma, provides a passage for water movement from the roots to the leaves [53]. Xylem vessels are hollow tubes [67] with thick lignified cell walls, which provide a low resistance pathway for water transport in vascular plants [68], and have no membranes or organelles [67]. Therefore, the wider the xylem vessel, the less resistance there is to water flow, thus the reduction observed in Lp xylem vessel size in this study may have a significant role in plant adaptation to water restriction, which facilitated water conduction within the plant [69].

Endodermis cell walls have a considerable role in grass species drought tolerance, as well as xylem vessels [70,71]. The root endodermis with casparian band are structurally specialised layers [70]. The endodermal casparian band prevents the apoplastic flow of ions from the cortex to the stele, and also prevents the flow of ions back from the apoplast of the stele to the apoplast of the cortex [72]. Ions carried by the proteins in the plasmalemma of the root epidermal and cortical cells enter to the stele [73]. As a result of the ion movement, the concentration of ions inside the endodermis is higher than that outside. Water naturally follows the concentration gradient to flow into the stele and xylem vessels, where water is channelled upwards to other parts of the plant.

## 5. Conclusions

In order to enhance water uptake and reduce water loss, plant tissue and cells often make adaptive changes and adjustments, which reflect their resistant strategy to soil water shortage and drought conditions. *Bromus valdivianus* had stronger capacities for water uptake and water storage when compared to Lp, due to its large root diameter, stele diameter and cortex thickness. Water restriction reduced root diameter, stele diameter, and cortex thickness, which negatively affected the ability of the root to capture and conserve water. In addition, similar to the tracheary element in the stele of Bv, Lp roots had aerenchyma in the cortex, which facilitated root ventilation. The enhancement of the pith cell wall was beneficial to water transport in Bv and Lp forage grasses under water restriction. Xylem lignifying and endodermis wall thickening enhance Lp drought resistance. These findings demonstrate that Bv and Lp have different individual structural and morpho-anatomical response strategies, which confer a degree of phenotypic plasticity in response to increasing soil water restriction. These strategies may allow them to enhance their survival and persistence under field conditions and increasing climate variability.

**Author Contributions:** Y.Z., J.G.-F., I.P.O., I.F.L., V.S. and P.D.K. conceptualisation; Y.Z., J.G.-F., H.H. and I.P.O. writing original draft preparation; Y.Z., J.G.-F., H.H., I.F.L., I.P.O., V.S. and P.D.K., methodology; I.F.L. and J.G.-F., statistics software and data analysis; I.F.L. and A.D.C., funding acquisition; I.F.L., A.D.C., V.S. and P.D.K., writing—review & editing. All authors have read and agreed to the published version of the manuscript.

**Funding:** This research received no external funding.

**Data Availability Statement:** Data are available upon request from the corresponding author.

**Acknowledgments:** We gratefully thank Xiongzhaoh He for his support in photomicrography, Xialin Zheng and Ying Wang for providing help in processing and analysing images, as well as to Lesly Taylor, Zhuo Yang, and Lulu He for their help and support at the Plant Growth Unit, Massey University. We thank Massey University Research Fund (MURF) and the T. R. Ellett Agricultural Research Trust for financial support.

**Conflicts of Interest:** The authors declare no conflicts of interest.

## References

- Lu, J.; Carbone, G.J.; Grego, J.M. Uncertainty and hotspots in 21st century projections of agricultural drought from CMIP5 models. *Sci. Rep.* **2019**, *9*, 4922–4934. [[CrossRef](#)]
- Cook, B.I.; Mankin, J.S.; Marvel, K.; Williams, A.P.; Smerdon, J.E.; Anchukaitis, K.J. Twenty-first century drought projections in the CMIP6 forcing scenarios. *Earth's Future* **2020**, *8*, e2019EF001461. [[CrossRef](#)]
- Ukkola, A.M.; Kauwe, M.G.D.; Roderick, M.L.; Abramowitz, G.; Pitman, A.J. Robust future changes in meteorological drought in cmip6 projections despite uncertainty in precipitation. *Geophys. Res. Lett.* **2020**, *47*, e2020GL087820. [[CrossRef](#)]
- Ziervogel, G.; Ericksen, P.J. Adapting to climate change to sustain food security. *Wiley Interdiscip. Rev. Clim. Change* **2010**, *1*, 525–540. [[CrossRef](#)]
- Thornton, P.K.; Ericksen, P.J.; Herrero, M.; Challinor, A.J. Climate variability and vulnerability to climate change: A review. *Glob. Change Biol.* **2014**, *20*, 3313–3328. [[CrossRef](#)] [[PubMed](#)]
- Vicente-Serrano, S.M.; Peña-Angulo, D.; Beguería, S.; Domínguez-Castro, F.; Tomás-Burguera, M.; Noguera, I.; Gimeno-Sotelo, L.; El Kenawy, A. Global drought trends and future projections. *Phil. Trans. R. Soc. A* **2022**, *380*, 20210285–20210308. [[CrossRef](#)]
- Malinowski, D.P.; Kigel, J.; Pinchak, W.E. Water deficit, heat tolerance, and persistence of summer-dormant grasses in the U.S. Southern plains. *Crop Sci.* **2009**, *49*, 2363–2370. [[CrossRef](#)]
- Godde, C.M.; Mason-D'Croz, D.; Mayberry, D.E.; Thornton, P.K.; Herrero, M. Impacts of climate change on the livestock food supply chain; a review of the evidence. *Glob. Food Secur.* **2021**, *28*, 100488–100505. [[CrossRef](#)]
- López, I.F.; Kemp, P.D.; Dörner, J.; Descalzi, C.A.; Balocchi, O.A.; García, S. Competitive strategies and growth of neighbouring *Bromus valdivianus* Phil. and *Lolium perenne* L. plants under water restriction. *J. Agron. Crop Sci.* **2013**, *199*, 449–459. [[CrossRef](#)]
- Makbul, S.; Güler, N.S.; Durmus, N.; Güven, S. Changes in anatomical and physiological parameters of soybean under drought stress. *Turk. J. Bot.* **2011**, *35*, 369–377. [[CrossRef](#)]
- Saha, P.; Sade, N.; Arzani, A.; Wilhelmi, M.M.R.; Coe, K.M.; Li, B.; Blumwald, E. Effects of abiotic stress on physiological plasticity and water use of *Setaria viridis* (L.) P. Beauv. *Plant Sci.* **2016**, *251*, 128–138. [[CrossRef](#)] [[PubMed](#)]
- Steudle, E. Water uptake by roots: Effects of water deficit. *J. Exp. Bot.* **2000**, *51*, 1531–1542. [[CrossRef](#)] [[PubMed](#)]
- Norton, M.R.; Malinowski, D.P.; Volaire, F. Plant drought survival under climate change and strategies to improve perennial grasses. A review. *Agron. Sustain. Dev.* **2016**, *36*, 29. [[CrossRef](#)]
- Volaire, F. A unified framework of plant adaptive strategies to drought: Crossing scales and disciplines. *Glob. Change Biol.* **2018**, *24*, 2929–2938. [[CrossRef](#)]
- Polania, J.A.; Poschenrieder, C.; Beebe, S.; Rao, I.M. Effective use of water and increased dry matter partitioned to grain contribute to yield of common bean improved for drought resistance. *Front. Plant Sci.* **2016**, *7*, 660. [[CrossRef](#)]
- Stone, E.L.; Kalisz, P.J. On the maximum extent of tree roots. *For. Ecol. Manag.* **1991**, *46*, 59–102. [[CrossRef](#)]
- Canadell, J.; Jackson, R.B.; Ehleringer, J.R.; Mooney, H.A.; Sala, O.E.; Schulze, E.D. Maximum rooting depth of vegetation types at the global scale. *Oecologia* **1996**, *108*, 583–595. [[CrossRef](#)]
- Schenk, H.J.; Jackson, R.B. The global biogeography of roots. *Ecol. Monogr.* **2002**, *72*, 311–328. [[CrossRef](#)]
- Schenk, H.J.; Jackson, R.B. Rooting depths, lateral root spreads and below-ground/above-ground allometries of plants in water-limited ecosystems. *J. Ecol.* **2002**, *90*, 480–494. [[CrossRef](#)]
- Peterson, R.L. Adaptations of root structure in relation to biotic and abiotic factors. *Can. J. Bot.* **1992**, *70*, 661–675. [[CrossRef](#)]
- Shao, H.B.; Chu, L.Y.; Jaleel, C.A.; Zhao, C.X. Water-deficit stress-induced anatomical changes in higher plants. *Comptes Rendus Biol.* **2008**, *33*, 215–225. [[CrossRef](#)] [[PubMed](#)]
- García-Favre, J.; López, I.F.; Cranston, L.M.; Donaghy, D.J.; Kemp, P.D. The growth response of pasture brome (*Bromus valdivianus* Phil.) to defoliation frequency under two soil-water restriction levels. *Agronomy* **2021**, *11*, 300. [[CrossRef](#)]
- Barkaouia, K.; Roumet, C.; Volaire, F. Mean root trait more than root trait diversity determines drought resilience in native and cultivated Mediterranean grass mixtures. *Agric. Ecosyst. Environ.* **2016**, *231*, 122–132. [[CrossRef](#)]
- Zwicke, M.; Picon-Cochar, C.; Morvan-Bertrand, A.; Prud'homme, M.-P.; Volaire, F. What functional strategies drive drought survival and recovery of perennial species from upland grassland? *Ann. Bot.* **2015**, *116*, 1001–1015. [[CrossRef](#)]
- Mostajeran, A.; Rahimi-Eichi, V. Drought stress effects on root anatomical characteristics of rice cultivars (*Oryza saliva* L.). *Pak. J. Agric. Sci.* **2008**, *11*, 2173–2183. [[CrossRef](#)]

26. Labdelli, A.; Adda, A.; Halis, Y.; Soualem, S. Effects of water regime on the structure of roots and stems of durum wheat (*Triticum durum* Desf.). *J. Bot.* **2014**, *2014*, 703874. [[CrossRef](#)]
27. Brent, D.B.; David, K.; Adam, J.L.; James, B. Evaluation of turf-type interspecific hybrids of meadow fescue with perennial ryegrass for improved stress tolerance. *Crop Sci.* **2014**, *54*, 355–365. [[CrossRef](#)]
28. García-Favre, J.; Cranston, L.M.; López, I.F.; Poli, C.H.E.C.; Donaghy, D.J.; Caram, N.; Kemp, P.D. Pasture brome and perennial ryegrass characteristics that influence ewe lamb dietary preference during different seasons and periods of the day. *Animal* **2023**, *17*, 100865–100874. [[CrossRef](#)]
29. Ordóñez, I.; López, I.F.; Kemp, P.D.; Descalzi, C.A.; Horn, R.; Zúñiga, F.; Dorota, D.; Dörner, J. Effect of pasture improvement managements on physical properties and water content dynamics of a volcanic ash soil in southern Chile. *Soil Tillage Res.* **2018**, *178*, 55–64. [[CrossRef](#)]
30. López, I.; Balocchi, O.; Lailhacar, P.; Oyarzún, C. Characterization of the growing sites of six native and naturalized species in the Humid Dominion of Chile. *Agro Sur* **1997**, *25*, 62–80. [[CrossRef](#)]
31. García-Favre, J.; López, I.F.; Cranston, L.M.; Donaghy, D.J.; Kemp, P.D.; Ordóñez, I.P. Functional contribution of two perennial grasses to enhance pasture production and drought resistance under a leaf regrowth stage defoliation criterion. *J. Agron. Crop Sci.* **2023**, *209*, 144–160. [[CrossRef](#)]
32. Ordóñez, I.P.; López, I.F.; Kemp, P.D.; Donaghy, D.J.; Dörner, J.; García-Favre, J.; Zhang, Y. A short-term effect of multi-species pastures and the plant's physiological response on pasture growth. *Eur. J. Agron.* **2024**, *159*, 127232. [[CrossRef](#)]
33. Ordóñez, I.P.; López, I.F.; Kemp, P.D.; Donaghy, D.J.; Zhang, Y.; Herrmann, P. Response of *Bromus valdivianus* (pasture brome) growth and physiology to defoliation frequency based on leaf stage development. *Agronomy* **2021**, *11*, 2058. [[CrossRef](#)]
34. Oliveira, B.A.; López, I.F.; Cranston, L.M.; Kemp, P.D.; Donaghy, D.J.; Dörner, J.; López-Villalobos, N.; García-Favre, J.; Ordóñez, I.P.; Van Hale, R. <sup>18</sup>O isotopic labelling and soil water content fluctuations validate the hydraulic lift phenomena for C<sub>3</sub> grass species in drought conditions. *Plant Stress* **2024**, *11*, 100414–100429. [[CrossRef](#)]
35. Zhang, Y.; García-Favre, J.; Hu, H.; López, I.F.; Ordóñez, I.P.; Cartmill, A.D.; Kemp, P.D. Aboveground structural attributes and morpho-anatomical response strategies of *Bromus valdivianus* Phil. and *Lolium perenne* L. to severe soil water restriction. *Agronomy* **2023**, *13*, 2964. [[CrossRef](#)]
36. Olmos, E.; Sanchez-Blanco, M.J.; Fernandez, T.; Alarcón, J.J. Subcellular effects of drought stress in *Rosmarinus officinalis*. *Plant Biol.* **2007**, *9*, 77–84. [[CrossRef](#)]
37. Descalzi, C.A.; López, I.F.; Kemp, P.D.; Dörner, J.; Ordóñez, I. Pasture restoration improvement methods for temperate degraded pastures and consequences of the climatic seasonality on soil–pasture complex. *J. Agron. Crop Sci.* **2020**, *206*, 130–147. [[CrossRef](#)]
38. Steel, R.G.D.; Torrie, J.H.; Dickey, D.A. *Principles and Procedures of Statistics: A Biometrical Approach*; McGraw-Hill: New York, NY, USA, 1997.
39. Descalzi, C.; Balocchi, O.; López, I.; Kemp, P.; Dörner, J. Different soil structure and water conditions affect the growing response of *Lolium perenne* L. and *Bromus valdivianus* Phil. growing alone or in mixture. *J. Soil Sci. Plant Nutr.* **2018**, *18*, 617–635. [[CrossRef](#)]
40. Zhang, Y.; Ma, H.; Calderón-Urrea, A.; Tian, C.; Bai, X.; Wei, J. Anatomical changes to protect organelle integrity account for tolerance to alkali and salt stress in *Melilotus officinalis*. *Plant Soil* **2016**, *406*, 327–340. [[CrossRef](#)]
41. Ruizin, S.E. *Plant Micro Technique and Microscopy*; Oxford University Press: Oxford, UK, 1999.
42. Jobson, J.D. *Applied Multivariate Data Analysis. Vol. II: Categorical and Multivariate Methods*; Springer: New York, NY, USA, 1996.
43. Shoaib, M.; Banerjee, B.P.; Hayden, M.; Kant, S. Roots' Drought Adaptive Traits in Crop Improvement. *Plants* **2022**, *11*, 2256. [[CrossRef](#)]
44. Dolezal, J.; Klimes, A.; Dvorsky, M.; Riha, P.; Klimesova, J.; Schweingruber, F. Disentangling evolutionary, environmental and morphological drivers of plant anatomical adaptations to drought and cold in Himalayan graminoids. *Oikos* **2019**, *128*, 1576–1587. [[CrossRef](#)]
45. Blum, A. Osmotic adjustment is a prime drought stress adaptive engine in support of plant production. *Plant Cell Environ.* **2017**, *40*, 4–10. [[CrossRef](#)] [[PubMed](#)]
46. Kapoor, D.; Bhardwaj, S.; Landi, M.; Sharma, A.; Ramakrishnan, M.; Sharma, A. The impact of drought in plant metabolism: How to exploit tolerance mechanisms to increase crop production. *Appl. Sci.* **2020**, *10*, 5692. [[CrossRef](#)]
47. Burks, J.; Tumber-Dávila, S.J. Rooted in potential: Advances in estimating spatiotemporal root water uptake in situ. *New Phytol.* **2025**. [[CrossRef](#)] [[PubMed](#)]
48. Ansari, S.A.; Kumar, P.; Gupta, B.N. Root surface area measurements based on adsorption and desorption of nitrite. *Plant Soil* **1995**, *175*, 133–137. [[CrossRef](#)]
49. Yan, M.; Zhang, L.; Ren, Y.; Zhang, T.; Zhang, S.; Li, H.; Chen, Y.; Zhang, S. The Higher Water Absorption Capacity of Small Root System Improved the Yield and Water Use Efficiency of Maize. *Plants* **2022**, *11*, 2300. [[CrossRef](#)]
50. Lüttge, U.; Laties, G.G. Selective inhibition of absorption and long distance transport in relation to the dual mechanisms of ion absorption in maize seedlings. *Plant Physiol.* **1967**, *42*, 181–185. [[CrossRef](#)]

51. Macklon, A.E.S.; Sim, A. Cortical cell fluxes and transport to the stele in excised root segments of *Allium cepa* L. IV. Calcium as affected by its external concentration. *Planta* **1981**, *152*, 381–387. [[CrossRef](#)]
52. Kotula, L.; Clode, P.L.; Striker, G.G.; Pedersen, O.; Läuchli, A.; Shabala, S.; Colmer, T.D. Oxygen deficiency and salinity affect cell-specific ion concentrations in adventitious roots of barley (*Hordeum vulgare*). *New Phytol.* **2015**, *208*, 1114–1125. [[CrossRef](#)]
53. Crang, R.; Lyons-Sobaski, S.; Wise, R. Parenchyma, collenchyma, and sclerenchyma. In *Plant Anatomy: A Concept-Based Approach to the Structure of Seed Plants*; Springer Nature: Cham, Switzerland, 2018; pp. 182–212.
54. Hose, E.; Clarkson, D.T.; Steudle, E.; Schreiber, L.; Hartung, W. The exodermis: A variable apoplastic barrier. *J. Exp. Bot.* **2001**, *52*, 2245–2264. [[CrossRef](#)] [[PubMed](#)]
55. Granse, D.; Titschack, J.; Ainouche, M.; Jensen, K.; Koop-Jakobsen, K. Subsurface aeration of tidal wetland soils: Root-system structure and aerenchyma connectivity in *Spartina* (Poaceae). *Sci. Total Environ.* **2022**, *802*, 149771. [[CrossRef](#)] [[PubMed](#)]
56. Mano, Y.; Omori, F. Breeding for flooding tolerant maize using “teosinte” as a germplasm resource. *Plant Root* **2007**, *1*, 17–21. [[CrossRef](#)]
57. Colmer, T.D. Long-distance transport of gases in plants: A perspective on internal aeration and radial oxygen loss from roots. *Plant Cell Environ.* **2003**, *26*, 17–36. [[CrossRef](#)]
58. Koop-Jakobsen, K.; Fischer, J.; Wenzhöfer, F. Survey of sediment oxygenation in rhizospheres of the saltmarsh grass—*Spartina anglica*. *Sci. Total Environ.* **2017**, *589*, 191–199. [[CrossRef](#)]
59. Kong, D.; Wang, J.; Zeng, H.; Liu, M.; Miao, Y.; Wu, H.; Kardol, P. The nutrient absorption–transportation hypothesis: Optimizing structural traits in absorptive roots. *New Phytol.* **2017**, *213*, 1569–1572. [[CrossRef](#)]
60. Katou, K.; Taura, T.; Furumoto, M. A model for water transport in the stele of plant roots. *Protoplasma* **1987**, *140*, 123–132. [[CrossRef](#)]
61. Blum, A. Effective use of water (EUW) and not water-use efficiency (WUE) is the target of crop yield improvement under drought stress. *Field Crops Res.* **2009**, *112*, 119–123. [[CrossRef](#)]
62. Xu, W.; Cui, K.; Xu, A.; Nie, L.; Huang, J.; Peng, S. Drought stress condition increases root to shoot ratio via alteration of carbohydrate partitioning and enzymatic activity in rice seedlings. *Acta Physiol. Plant.* **2015**, *37*, 9–20. [[CrossRef](#)]
63. Pace, P.F.; Cralle, H.T.; El-Halawany, S.H.M.; Cothren, J.T.; Senseman, S.A. Drought-induced changes in shoot and root growth of young cotton plants. *J. Cotton Sci.* **1999**, *3*, 183–187.
64. Huang, B.R.; Fry, J.D. Root anatomical, physiological, and morphological responses to drought stress for tall fescue cultivars. *Crop Sci.* **1998**, *38*, 1017–1022. [[CrossRef](#)]
65. Pirnajmedin, F.; Majidi, M.M.; Saeidi, G.; Gheysari, M.; Volaire, F.; Barre, P.; Osivand, A.H.; Sarfaraz, D. Persistence, recovery and root traits of tall fescue genotypes with different flowering date under prolonged water stress. *Euphytica* **2017**, *213*, 269. [[CrossRef](#)]
66. Wang, Y.; Meng, B.; Zhong, S.; Wang, D.; Ma, J.; Sun, W. Aboveground biomass and root/shoot ratio regulated drought susceptibility of ecosystem carbon exchange in a meadow steppe. *Plant Soil* **2018**, *432*, 259–272. [[CrossRef](#)]
67. Kozela, C.; Regan, S. How plants make tubes. *Trends Plant Sci.* **2003**, *8*, 159–164. [[CrossRef](#)] [[PubMed](#)]
68. Barceló, A.R. Xylem parenchyma cells deliver the H<sub>2</sub>O<sub>2</sub> necessary for lignification in differentiating xylem vessels. *Planta* **2005**, *220*, 747–756. [[CrossRef](#)] [[PubMed](#)]
69. Sun, Y.; Robert, C.A.M.; Thakur, M.P. Drought intensity and duration effects on morphological root traits vary across trait type and plant functional groups: A meta-analysis. *BMC Ecol. Evol.* **2024**, *24*, 92–103. [[CrossRef](#)]
70. Wang, P.; Calvo-Polanco, M.; Rey, G.; Barberon, M.; Champeyroux, C.; Santoni, V.; Maurel, C.; Franke, R.B.; Ljung, K.; Novak, O.; et al. Surveillance of cell wall diffusion barrier integrity modulates water and solute transport in plants. *Sci. Rep.* **2019**, *9*, 4227–4238. [[CrossRef](#)]
71. Dabravolski, S.A.; Isayenkov, S.V. The regulation of plant cell wall organisation under salt stress. *Front. Plant Sci.* **2023**, *14*, 1118313–1118329. [[CrossRef](#)]
72. Enstone, D.E.; Peterson, C.A.; Ma, F. Root endodermis and exodermis: Structure, function, and responses to the environment. *J. Plant Growth Regul.* **2003**, *21*, 335–351. [[CrossRef](#)]
73. Viana, W.G.; Scharwies, J.D.; Dinneny, J.R. Deconstructing the root system of grasses through an exploration of development, anatomy and function. *Plant Cell Environ.* **2022**, *45*, 602–619. [[CrossRef](#)]

**Disclaimer/Publisher’s Note:** The statements, opinions and data contained in all publications are solely those of the individual author(s) and contributor(s) and not of MDPI and/or the editor(s). MDPI and/or the editor(s) disclaim responsibility for any injury to people or property resulting from any ideas, methods, instructions or products referred to in the content.